Received: 24 October 2019 | Revised: 20 December 2019 | Accepted: 20 December 2019

DOI: 10.1111/jace.16979

ORIGINAL ARTICLE

Journal of the American Ceramic Society

Modeling nonisothermal crystallization in a $BaO \bullet 2SiO_2$ glass

D. C. Van Hoesen[1] | **Xinsheng Xia**[2] | **Matthew E. McKenzie**[3] | **K. F. Kelton**[1,2]

[1]Department of Physics, Washington University, St. Louis, MO, USA

[2]Institute of Materials Science and Engineering, Washington University, St. Louis, MO, USA

[3]Science and Technology Division, Corning Incorporated, Corning, NY, USA

Correspondence
Danniel C. Van Hoesen, Department of Physics, Washington University, St. Louis, MO, USA.
Email: d.vanhoesen@wustl.edu

Funding information
National Science Foundation, Grant/Award Number: DMR 17-20296; Corning Inc

Abstract

The accuracy of a differential thermal analysis (DTA) technique for predicting the temperature range of significant nucleation is examined in a $BaO \bullet 2SiO_2$ glass by iterative numerical calculations. The numerical model takes account of time-dependent nucleation, finite particle size, size-dependent crystal growth rates, and surface crystallization. The calculations were made using the classical and, for the first time, the diffuse interface theories of nucleation. The results of the calculations are in agreement with experimental measurements, demonstrating the validity of the DTA technique. They show that this is independent of the DTA scan rate used and that surface crystallization has a negligible effect for the glass particle sizes studied. A breakdown of the Stokes-Einstein relation between viscosity and the diffusion coefficient is demonstrated for low temperatures, near the maximum nucleation rate. However, it is shown that accurate values for the diffusion coefficient can be obtained from the induction time for nucleation and the growth velocity in this temperature range.

KEYWORDS

barium silicate glasses, differential scanning calorimetry, differential thermal analysis, nucleation, simulation

1 | INTRODUCTION

A quantitative knowledge of the time-dependent nucleation rate as a function of temperature, $I(t,T)$, is critically important for developing new glasses and for preparing glass ceramics with a desired microstructure. If the temperature ranges for nucleation and growth are sufficiently separated, $I(t,T)$ can be accurately measured using a two-step heat treatment method. Nuclei are first developed by heating for different amounts of time in a temperature range where the nucleation rate is significant (nucleation treatment). These nuclei are subsequently grown to observable crystals with a heat treatment at a higher temperature, where the growth rate is significant (growth treatment). The steady-state nucleation rate and the transient time for nucleation can be determined from the number of crystals produced as a function of the isothermal heating time at the nucleation temperature.[1]

Nucleation measurements made using this two-step method are very time consuming, requiring many weeks or even months to obtain a complete set of data. Further, for such measurements to even be feasible, a prior knowledge of the temperature range where significant nucleation occurs is required. As suggested previously from studies of crystallization in lithium disilicate glasses,[2–4] thermal analysis methods such as differential thermal analysis (DTA) and differential scanning calorimetry (DSC) can be used to determine this. This was also recently experimentally confirmed in two barium-silicate glasses[5]. Ray et al[6] and Ranasinghe et al[7] argued that the DTA/DSC method can be used to quantitatively measure the nucleation rate. However, this technique was critically reviewed and refined by Fokin et al[8] who found that it could only give accurate quantitative nucleation rate data if a significant amount of preliminary data were known. The DTA/DSC method has been examined numerically for the lithium silicate glasses assuming the classical theory of nucleation (CNT) and demonstrated to be valid.[9,10] However, no numerical investigation has been made for other silicate glasses. Here the accuracy of the DTA/DSC technique to find

the temperature region of significant nucleation is examined by numerical modeling in a barium silicate ($BaO{\bullet}2SiO_2$) glass. It should be emphasized that it is not the purpose of the investigation to determine whether the DTA technique can be used to obtain quantitative information on the nucleation rate data.

Two models are used to describe the time-dependent nucleation behavior, the CNT and a more recently developed model, the diffuse interface theory (DIT).[11–13] The CNT based calculations describe the DTA only if at low temperatures the work of critical cluster formation is radically different from the form that is expected.[14,15] A similar anomalous behavior was also noted by Xia et al[16] in experimental measurements of the steady-state nucleation rate and transient times using a two-step heating method. The steady-state rate was much smaller than predicted by the CNT for temperatures below that of the peak nucleation rate. For those measurements, the possibility was left open that the heating times at the nucleation temperature were too short to reach the steady-state. The DTA calculation was used to try to resolve this possibility. The anomalous work of cluster formation was examined in terms of a nonlinear change in the driving free energy as a function of temperature, a nonlinear change in the interfacial width as a function of temperature, or a breakdown of the CNT. A possible nonlinear change in the interfacial free energy as a function of temperature is not considered here. Two methods were used to calculate the driving free energy used in the CNT, (i) the Turnbull approximation and (ii) the values obtained by forcing the CNT to fit to the anomalous low temperature nucleation data. For the DIT fits, the interfacial width was either taken to be linear, giving similar steady-state nucleation rates as the CNT when the Turnbull approximation is used, or to have a temperature dependence described by a piecewise linear fit obtained when the calculated rates were forced to agree with the measured nucleation data, giving similar steady-state nucleation rates as the CNT when the anomalous driving free energy is used. Unfortunately, the DTA method was not sufficiently sensitive to obtain a clear answer to the question of the anomalous low temperature nucleation data. However, the DIT calculations showed that the experimental data indicate an increase in the interfacial width between the nucleating cluster and the parent glass phase with decreasing temperature, which is not considered within the CNT.

2 | NUMERICAL MODEL

As mentioned, the classical and diffuse interface theories of nucleation are used to model the DTA data. A brief description of the model is given here; a more detailed description can be found elsewhere.[2,9,17–21]

The CNT and the DIT differ in the way in which the work required to form a crystal cluster, $W(n)$, is calculated. Assuming spherical clusters, within the CNT gives

$$W(n) = n\Delta\mu + \left(36\pi\bar{v}^2 n^2\right)^{1/3}\sigma, \tag{1}$$

where $\Delta\mu$ is the difference in the Gibbs free energies of the glass and crystal phases per formula unit (hereon referred to as a *monomer*), σ is the interfacial free energy, $\bar{v}$ is the volume of a monomer, and n is the number of monomers in the cluster. In deriving this expression, it is assumed that there is a sharp interface between the nucleating cluster and the original phase. Density functional calculations show that this is an inaccurate picture[22]. The actual interface is diffuse, constituting a large fraction of the cluster diameter when nucleation occurs far from equilibrium, as is the case for glass crystallization. A phenomenological model to take the diffuse interface into account was proposed independently by Gránásy[11,12] and Spaepen.[13] Within the DIT, the work of cluster formation is expressed in terms of the Gibbs free energy as a function of distance from the cluster center,

$$W = \int_0^\infty 4\pi r^2 g(r)\, dr, \tag{2}$$

where $g(r) = \Delta h - T\Delta s$, with Δh, the enthalpy difference between the glass and crystal, and Δs, the entropy difference between the glass and crystal. Within the DIT $g(r)$, Δh, and Δs are expressed by a series of step functions that define the interface width.

The difference between the CNT and the DIT is then in the thermodynamic model; the kinetics are assumed to follow those of the CNT. In this model, the clusters evolve one monomer at a time, following the bimolecular reactions as shown in Figure 1. From this, the rate of change of the cluster population of size n at time t, $N_{n,t}$, is given by

$$\frac{dN_{n,t}}{dt} = N_{n-1,t}k_{n-1}^{+} + N_{n+1,t}k_{n+1}^{-} - N_{n,t}k_{n}^{-} - N_{n,t}k_{n}^{+}, \tag{3}$$

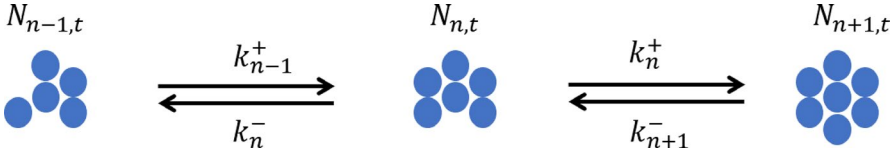

FIGURE 1 The bimolecular reaction controlling the cluster size n at time t, where $N_{n,t}$ is the cluster population density, k_n^+ is the forward reaction rate, and k_n^- is the backward reaction rate

where k_n^+ and k_n^- are the forward and backward reaction rates at cluster size n,

$$k_n^+ = \frac{6D}{\lambda^2} O_n \exp\left(-\frac{W_{n+1} - W_n}{2k_B T}\right)$$
$$k_n^- = \frac{6D}{\lambda^2} O_{n-1} \exp\left(+\frac{W_{n+1} - W_n}{2k_B T}\right). \quad (4)$$

Here, D is the diffusion coefficient in the glass/liquid, λ is the atomic jump distance, and O_n is the number of attachment sites (equal to $4n^{2/3}$ for a spherical cluster containing n monomers).

The time-dependent cluster population can be obtained using a finite difference method, in which the time is divided up into small increments, δt.

$$N_{n,t+dt} = N_{n,t} + \delta t \left(\frac{dN_{n,t}}{dt}\right). \quad (5)$$

With the results of the iteration the time-dependent nucleation rate, $I_{n,t}$, is readily computed at any cluster size n, since it is the flux of clusters growing or shrinking past that size

$$I_{n,t} = N_{n,t} k_n^+ - N_{n+1,t} k_{n+1}^-. \quad (6)$$

To model the nonisothermal crystallization of the glass in DTA, it is necessary to calculate the growth rate as a function of cluster size. The growth of very small clusters, near the critical size for nucleation, is stochastic.[23] However, when the clusters are sufficiently large, they transition to growth kinetics, which are well described by an expression due to Kelton and Greer,[18]

$$\frac{dr}{dt} = \frac{16D}{\lambda^2}\left(\frac{3\bar{v}}{4\pi}\right)^{1/3} \sinh\left[\frac{\bar{v}}{2k_B T}\left(\Delta G_v - \frac{2\sigma}{r}\right)\right], \quad (7)$$

where ΔG_v is the free energy decrease per unit volume on crystallization and k_B is the Boltzmann constant. Often D is computed from the measured viscosity using the Stokes-Einstein equation. However, it has been shown that the Stokes-Einstein equation breaks down above the glass transition temperature.[24] The breakdown for $BaO{\bullet}2SiO_2$ occurs near 1140K[25] (1.18 T_g) which is approximately equal to the DTA crystallization peak maximum temperature (see Figure 4 and Figure 7 respectively). Here we show additional evidence of this breakdown in the DTA results. The diffusion coefficient can also be obtained from experimental measurements of the induction time[16] or experimental measurements of the growth velocity for macroscopic crystals.[25] Following the work of Kashchiev,[26] the diffusion coefficient computed from the induction time, Θ, is.

$$D = \frac{k_B T \lambda^2 n^{*1/3}}{6\Theta\,|\Delta\mu|}, \quad (8)$$

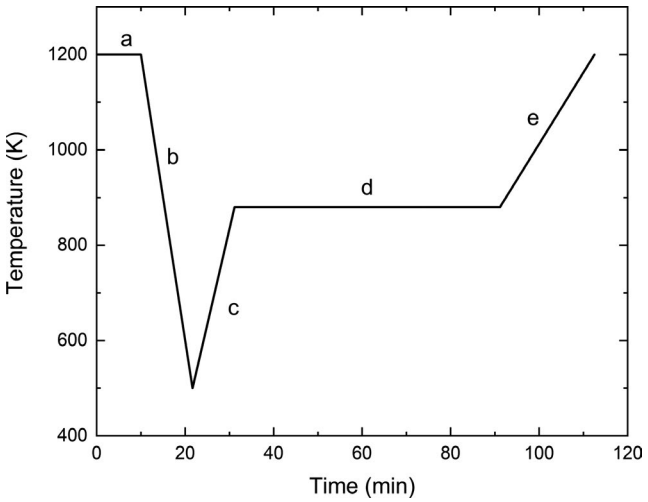

FIGURE 2 An example of the profile used in the experimental measurements and the simulations. The steps are: (a) establish an equilibrium distribution at a high temperature; (b) quench the system at 60 K/min to a low temperature; (c) heat at 40 K/min to the nucleation temperature; (d) isothermally heat for 60 minutes; (e) scan at 15 K/min through the crystallization peak

TABLE 1 Temperature-independent parameters used in the simulations

Parameter	Symbol	Units	$BaO{\bullet}2SiO_2$
Liquidus temperature	T_l	K	1693
Heat of fusion	ΔH_f	kJ mol^{-1}	37.5
Monomer volume	$\bar{v}$	m^3	1.216×10^{28}
Jump distance	λ	Å	$\bar{v}^{1/3} = 4.954$

where n^* is the critical cluster size, beyond which clusters tend to grow, and $\Delta\mu$ is the driving free energy for a single monomer. Equation 7 can be used to obtain the diffusion coefficient from growth velocity data.

For each time step, δt, the extended volume transformed (assuming no overlap of the transformed regions) is calculated as

$$x_e(t) = \frac{1}{v}\sum_{i=l}\frac{4\pi}{3} N_i r_{i,t}^3, \quad (9)$$

where v is the total volume, N_i is the population of the cluster or nuclei at size i, $r_{i,t}$ is the radius of the cluster or nuclei at size i at the time of the calculation, t, and l is the lower limit on the cluster size distribution. The lower limit is set to nine monomers in the simulations, since this can be argued to be the smallest configuration that would not occur in the equilibrium glass. The actual volume fraction transformed as a function of time, $x(t)$, must take into account the overlap between crystals. Assuming that the crystals form by homogeneous nucleation (so that they appear randomly in space and time) and that the sample size may be taken to be infinite, the Johnson-Mehl-Avrami-Kolmogorov (JMAK) method[27–31] allows $x(t)$ to be computed from $x_e(t)$,

$$x(t) = 1 - \exp\left(-x_e(t)\right). \quad (10)$$

Since powder samples are typically used for the DTA experiments, they cannot be assumed to be infinite in size. Instead, corrections for the finite particle size effects follow the method discussed by Levine.[21] It was found in studies of lithium disilicate glass that for powders with particle sizes greater than 300 μm internal crystallization controls the location of the peak temperature and surface crystallization matters very little.[4] The DTA experiments on barium disilicate glasses, used powders with an average particle size of 526 μm with a 400 μm lower limit.[5] For the numerical calculations an even distribution of particle sizes with the same range and an upper limit of 652 μm was assumed. Additionally, the internal nucleation rate at the maximum nucleation rate temperature for barium disilicate[16,32,33] is greater than 300 times larger than that of lithium disilicate,[32,34–36] suggesting that for larger particles and faster internal nucleation rates, surface crystallization should not have a strong influence. To check this, surface crystallization was also included in the numerical calculation in the following way. First, it was assumed that surface nucleation was very fast, quickly leading to a surface crystallization shell around the particle during the quench. The shell was allowed to grow inward, toward the particle center, with the measured surface growth velocity[25] (which is approximately 1.27 times the internal growth velocity). While it is unknown if the surface nucleation is sufficiently fast to create a complete surface layer during the quench, this assumption gives the maximum possible effect due to surface nucleation and growth.

The measured DTA signal reflects the amount of heat (enthalpy) released during crystallization. Assuming that this is proportional to the volume transformed, the DTA signal can be calculated as.

$$\text{DTA signal} \propto \frac{x(t_i+\delta t)-x(t_i)}{\delta t}. \quad (11)$$

The temperature profile used in the DTA experiments is adopted for the numerical calculations, an example of which is shown in Figure 2.

3 | RESULTS AND DISCUSSION

The driving free energy and the interfacial free energy are key parameters in the CNT. Two methods were used to extract them from the experimental measurements of the steady-state nucleation rates. In the first method the driving free energy was calculated as

$$\Delta G = \frac{\Delta H_f (T - T_l)}{T_l}, \quad (12)$$

where ΔH_f is the heat of fusion, T is the temperature, and T_l is the liquidus temperature (often called the Turnbull approximation). A more accurate calculation of the driving free energy

TABLE 2 Diffusion coefficient dependent parameters used in the simulations, determined by matching the calculated steady-state nucleation rate to the experimentally measured rate

Parameter	Symbol	Units	Growth velocity	Induction time	Stokes-Einstein
Diffusion coefficient	$\log_{10}(D_0)$	$m^2\ s^{-1}$	−13.005	−11.130	–
	A	unitless	−750.501	−256.705	–
	τ	K	219.141	307.427	–
Viscosity (KKZNT)	$\log_{10}(\eta_0)$	Pa s	–	–	−5.427
	E_∞	K	–	–	10423
	B	unitless	–	–	67.98
	T^*	K	–	–	1456.6
Interfacial free energy	σ_0	$J\ m^{-2}$	0.06995	0.07383	0.04281
	σ_1	$J\ m^{-2}\ K^{-1}$	3.707×10^{-5}	3.266×10^{-5}	6.187×10^{-5}
Gibb's driving free energy	a	$kJ\ m^{-3}$	−198740	−159790	−197130
	k_1	$kJ\ m^{-3}\ K^{-1}$	−17.656	−57.33	−19.542
	k_2	$kJ\ m^{-3}\ K^{-1}$	303.01	302.825	303.279
	T_i	K	978.80	979.102	978.053
Interface width	a	Å	5.7459	6.205	4.9116
	k_1	$ÅK^{-1}$	−0.0031	−0.00358	−0.00232
	k_2	$ÅK^{-1}$	-3.487×10^{-4}	-4.525×10^{-4}	2.948×10^{-4}
	T_i	K	978.8	978.99	978.1

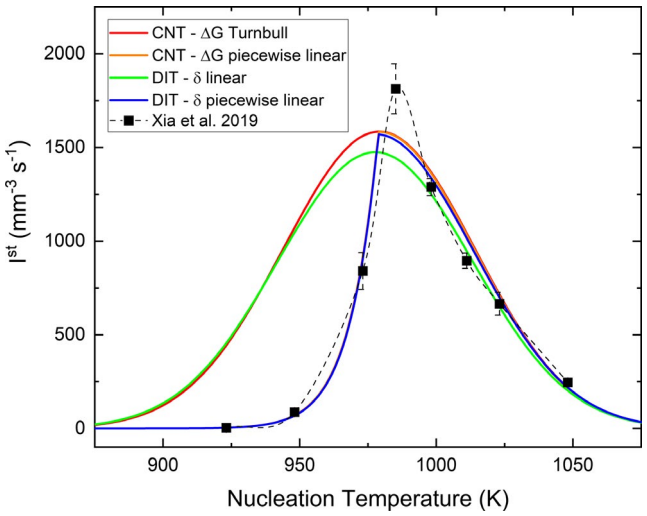

FIGURE 3 The calculated steady-state nucleation rates for the methods discussed using the diffusion coefficient obtained from growth velocity are compared with the experimental data

could be made if the specific heats of the crystal and glass were known. However, while this would change the value quantitatively, qualitatively the driving free energy would still be the same. The interfacial free energy was obtained by matching the fit of the high temperature steady-state nucleation rate data to the rate predicted by CNT. While these give good fits at high temperature, anomalies appear at low temperatures. The source of the anomalies is of current debate. Experimental and theoretical considerations show that the interfacial free energy increases linearly with increasing temperature.[1] Assuming this, the second method obtains the interfacial free energy at low temperatures from an extrapolation of the high temperature values. The driving free energy is then computed by forcing agreement between the steady-state nucleation rate predicted by CNT and the measured value. In the first method, the Turnbull approximation is used and the interfacial free energy is assumed to be linear. For this to be true, the measured steady-state nucleation rate data[16,32,33] would have to be incorrect, which could be the case if steady-state were not achieved during the two-step heating treatment. The second method assumes that the steady-state is achieved and that either the CNT breaks down or the driving free energy behaves anomalously at temperatures below the maximum nucleation rate temperature. Values obtained from both methods were used to calculate the DTA curves using the CNT.

The DTA scans were also calculated using the diffuse interface theory, presuming that the anomalous behavior of the nucleation rate at low temperature is real and reflects a failure of the CNT. In the first DIT method, the width of the interface was adjusted in a piecewise linear fit to force the experimental data to match the values predicted by the DIT. Assuming that the measured steady-state nucleation rate data at low temperatures are lower than the real steady-state values, the interface width that was obtained at high

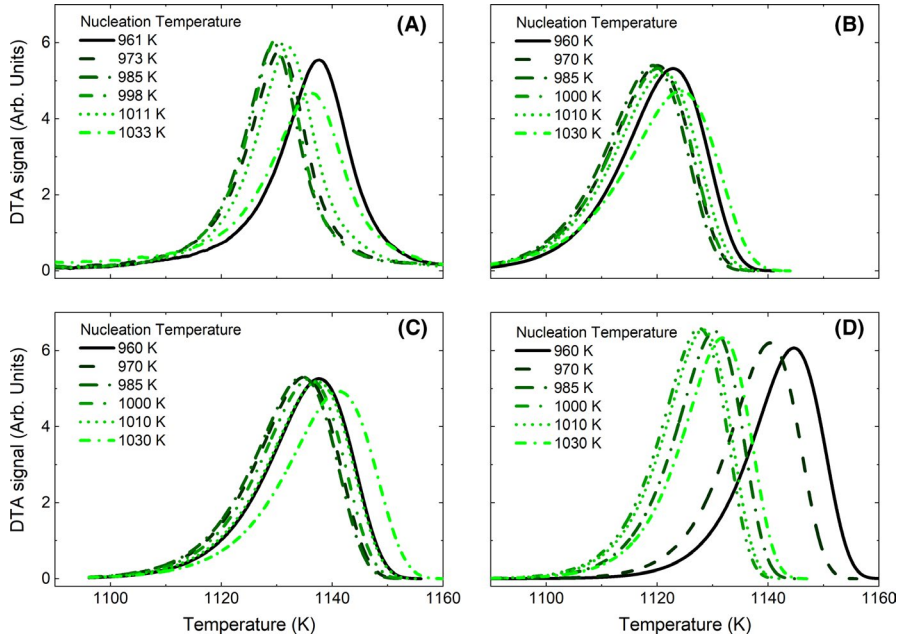

FIGURE 4 The calculated DTA signals during a 15 K/min scan after one hour of isothermal heating at various temperatures (listed in the legend) neglecting surface crystallization: (A) experimental data; (B) numerical calculation for the CNT, calculating the driving free energy from the Turnbull approximation, and calculating the diffusion coefficient from the growth velocity; (C) numerical calculation for the CNT, calculating the driving free energy from the Turnbull approximation, and calculating the diffusion coefficient from the induction time; (D) numerical calculation for the CNT, calculating the driving free energy from the Turnbull approximation, and calculating the diffusion coefficient from the viscosity using the Stokes-Einstein relation

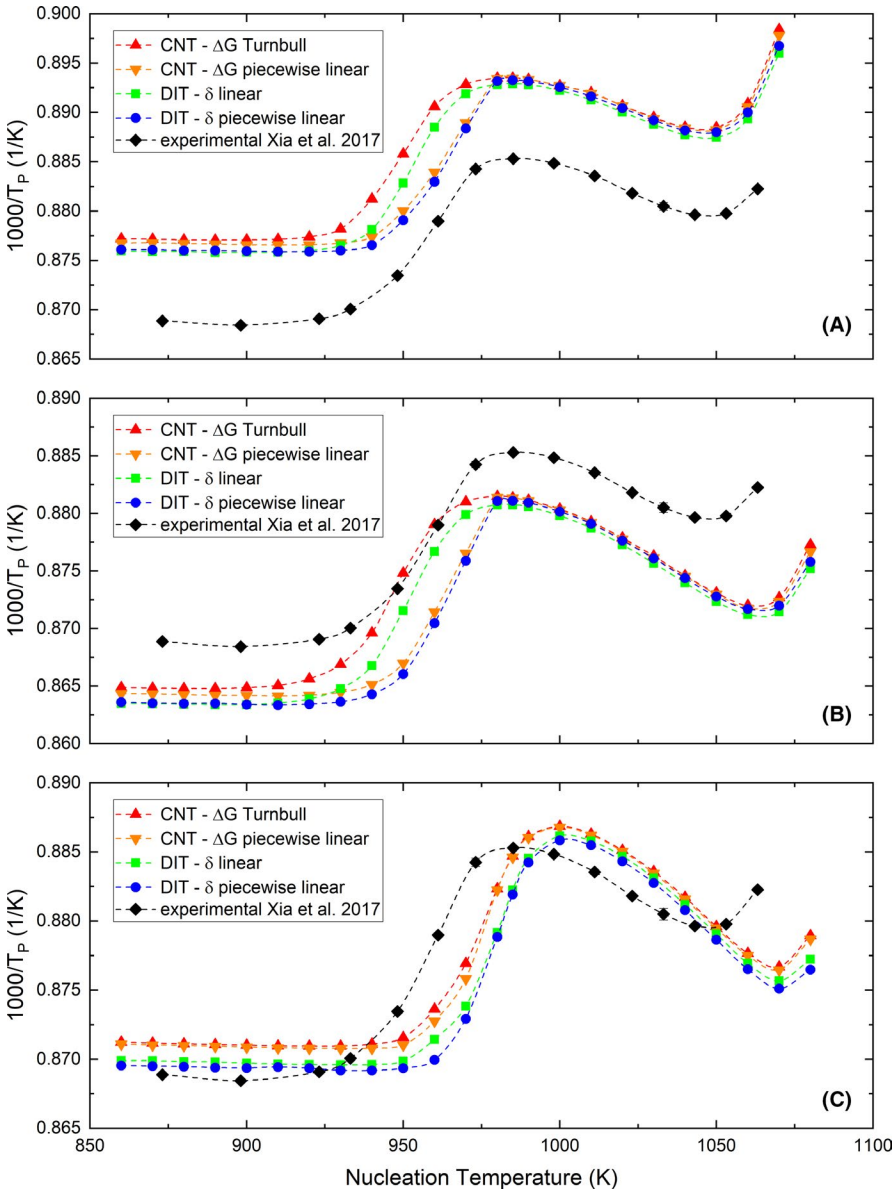

FIGURE 5 The inverse peak temperature for the experimental and numerical DTA data for the $BaO{\bullet}2SiO_2$ glass with (A) the diffusion coefficient calculated from the growth velocity; (B) the diffusion coefficient calculated from the induction time; (C) the diffusion coefficient calculated from the viscosity assuming the Stokes-Einstein relation. The errors in the experimental data are the size of the symbols[5]. The propagated errors in the numerical DTA data from the diffusion coefficient produce differences in the data smaller than the size of the symbols

temperatures by forcing a match between the experimental steady-state data with those calculated from the DIT was extrapolated to low temperatures in a linear fit for the second DIT method.

Table 1 lists the temperature-independent parameters used in the simulations, which were obtained from the literature[1]. These include the liquidus temperature, the heat of fusion, the monomer volume, and the atomic jump distance. Table 2 lists the parameters required to match the experimental steady-state nucleation rate data to the calculated steady-state nucleation rate data for each diffusion coefficient used in the simulations. The diffusion coefficient calculated from the growth velocity and induction time has the form

$$\log_{10}(D) = \log_{10}(D_0) + A exp\left(-\frac{T}{\tau}\right), \quad (13)$$

where D_0, A, and τ are fitting parameters. The validity of the Stokes-Einstein equation was assumed to calculate the diffusion coefficient from the viscosity. The avoided critical point model (KKZNT)[37–39] was used to fit the viscosity data,

$$\log_{10}(\eta) = \log_{10}(\eta_0) + \frac{1}{T}\left[E_\infty + T^* B\left(\frac{T^*-T}{T^*}\right)^{8/3}\theta(T^*-T)\right] \quad (14)$$

where η_0, E_∞, B, and T^* are fitting parameters. The diffusion coefficient is then

$$D = \frac{k_B T}{6\pi\eta r}, \quad (15)$$

where r is the monomer radius. Other parameters in Table 2 use either the diffusion coefficient obtained from the growth velocity, the induction time, or the viscosity to match the steady-state nucleation rate data. The interfacial free energy is taken to be

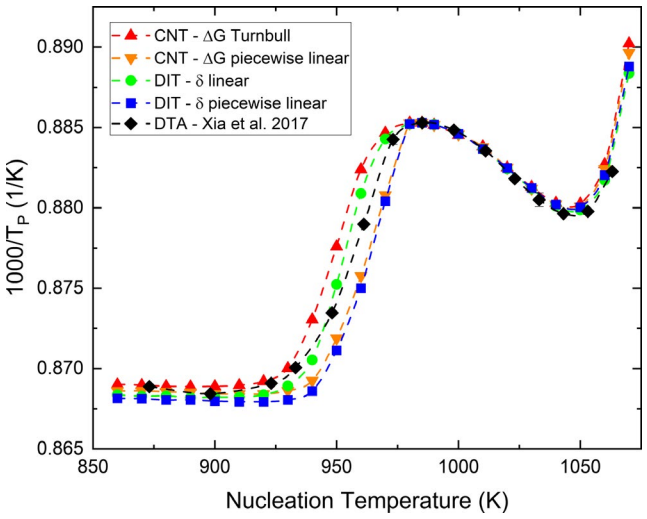

FIGURE 6 The inverse peak temperature for the experimental and calculated DTA data for the $BaO{\bullet}2SiO_2$ glass. The numerical calculation has been shifted to match the experimental data at a single data point, 985 K

linear with temperature, $\sigma = \sigma_0 + \sigma_1 T$. Both the Gibb's driving free energy, ΔG, and the interfacial width, δ, are fit with piecewise linear functions of the form

$$\Delta G, \delta = \begin{cases} a + k_1 T & \text{for } T < T_i \\ a + k_1 T_i + k_2 \left(T - T_i\right) & \text{for } T \geq T_i \end{cases}, \quad (16)$$

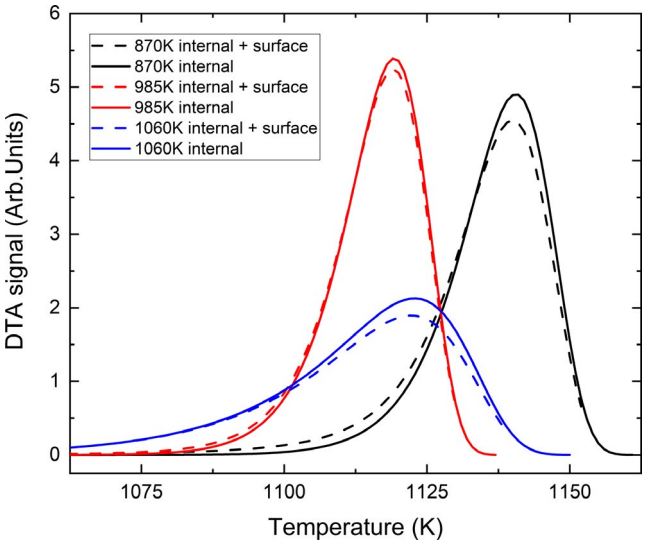

FIGURE 7 The calculated DTA signals during a 15 K/min scan after one hour of isothermal heating at various temperatures (listed in the legend) for simulations when internal and surface nucleation and growth are taken into account (dashed lines) and when only internal nucleation and growth are present (solid lines)

where a, k_1, k_2, and T_i are fitting parameters. The driving free energy at high temperatures follows the Turnbull approximation, as previously mentioned.

The calculated nucleation rates as a function of temperature for the two methods assumed for the CNT and the DIT, using the diffusion coefficient calculated from the growth velocity, are compared with recent experimental measurements by Xia[16] in Figure 3. The calculations using the Turnbull approximation in the CNT and the linear interface width in the DIT match the experimental data at high temperatures but deviate at low temperatures. The quality of the fit in the calculations using the piecewise linear driving free energy in the CNT and the piecewise linear interface width in the DIT, as well as the high temperature portions of the other two calculations, reflects the quality of the fit parameters.

Shown in Figure 4 are several selected experimental DTA curves for $BaO{\bullet}2SiO_2$ glasses for different nucleation temperatures (A),[5] and the numerical results obtained using the CNT along with the Turnbull approximation for the driving free energy and the three methods for determining the diffusion coefficients (B-D). There are several sources of error that must be considered to account for the differences in the experimental DTA curves and the numerically calculated ones. The diffusion coefficient controls both the nucleation and growth of the clusters. As observed in Figure 4, the choice of diffusion coefficient makes a large difference in the DTA curves. Additionally, The $BaO{\bullet}2SiO_2$ glass is known to form irregularly shaped crystals at some temperatures.[16,33] If the crystals are irregularly shaped, then the assumption of spherical growth in the simulation will give an overestimate for the extended volume transformed. Accounting for the irregularly shaped crystals increases the peak temperature and decrease the peak width because the growth rate is larger at higher temperatures. A rough estimate for the real volume fraction transformed due to the irregularly shaped crystals was made from the $BaO{\bullet}2SiO_2$ image in the manuscript by Xia.[16] When the growth velocity is used to calculate the diffusion coefficient, the peaks in the DTA scan shift by 5K higher in temperature, becoming more similar to the experimental data. This shift would account for half the vertical offset in the numerical and the experimental data in Figure 5A. Also, since the simulation uses the fits to the experimental data to determine the driving free energy, the interfacial free energy, and the interface width, the predicted steady-state nucleation rates may be incorrect at low temperatures.

As discussed in the introduction, several studies have shown that differential thermal analysis (DTA) and differential scanning calorimetry (DSC) measurements can be used to determine the temperature range for significant nucleation.[4–7,40] Most recently the DTA technique was used to estimate this for $BaO{\bullet}2SiO_2$ and $5BaO{\bullet}8SiO_2$ glasses[5]; it

was determined that the inverse peak temperature from the DTA scans for different nucleation temperatures gave the best estimates. A comparison between those experimental DTA data for $BaO{\bullet}2SiO_2$ and the numerical calculations made as a function of the nucleation temperature using the three methods previously described is given in Figure 5.

The inverse peak temperature as a function of the nucleation temperature in the DTA data that were numerically calculated using both the CNT and DIT agree well with the experimental data when the diffusion coefficient is calculated from the growth velocity and from the induction time. Most importantly, the maximum in the inverse peak temperature agrees with the maximum nucleation rate measurement and the experimental inverse peak temperature maximum. In contrast, the calculated DTA values based on the viscosity and assuming the Stokes-Einstein relation are in striking disagreement with the experimental data. This provides additional strong evidence for the breakdown of the Stokes-Einstein equation for temperatures near the crystallization temperature. It is less clear, however, which nucleation theory compares best to the experimental data. To investigate this question the calculated inverse peak temperature for the maximum nucleation rate was matched to the experimentally measured value. The diffusion coefficient used for the numerical calculations was obtained from the measured growth velocity. As observed in Figure 6, the agreement between the calculated and measured data is very good for temperatures above the peak nucleation temperature, indicating that theories examined are all in good agreement at high temperatures. However, for temperatures less than the maximum nucleation rate temperature, they disagree and there is no clear indication of a better model.

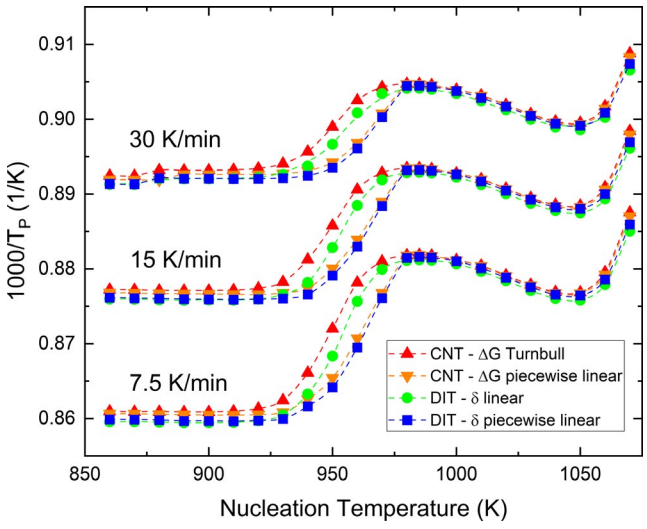

FIGURE 8 The inverse peak temperature of the calculated DTA data for the $BaO{\bullet}2SiO_2$ glass using three different DTA scan rates. The predicted temperature range for significant nucleation is the same

A failure of the CNT to fit time-dependent nucleation data at temperatures lower than that of the peak nucleation rate was reported by Xia et al.[16] This is similar to behavior reported earlier in other silicate glasses where a changing size of the structural units, spatial heterogeneity and dynamical heterogeneity have been proposed to explain these results,[15,41–43] but the question still remains unclear. A recent publication suggests that the failure may be an experimental artifact arising from insufficient time in the experiments for steady-state to be reached.[44] Unfortunately, the DTA calculations discussed here do not appear to be sensitive enough to support or oppose the validity of the experimental time-dependent nucleation results.

The numerical calculations show that for the particle size used, surface crystallization plays no role in determining the peak temperature during the DTA scan. Figure 7 shows the calculated DTA signals for three different temperatures with and without surface crystallization. Changes in the peak temperatures are negligible and changes in the magnitude of the peaks are extremely small. Even though the surface layer is numerically determined to be between 3% and 10% of the particle diameter for 526 μm particles, surface crystallization plays no role in determining the peak temperature during the simulated DTA scan. The thickness of the crystallization layers in the DTA simulations is near 20 μm for low nucleation treatment temperatures, drops to 8 μm for nucleation treatment temperatures near the maximum internal nucleation rate temperature, and then rises to 27 μm for the highest nucleation treatment temperature. As previously stated, these surface layer thicknesses are

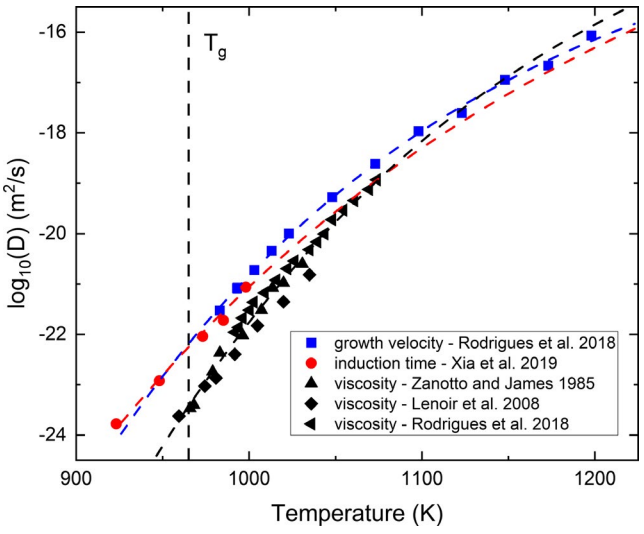

FIGURE 9 The calculated diffusion coefficient as a function of temperature from experimental measurements of the viscosity, the induction time, and the growth velocity. The fits used in the DTA simulations are shown as dashed lines, taking the parameters from Table 2. The errors for the diffusion coefficient calculated from the growth velocity and induction time are smaller than the size of the symbols. The error in the viscosity was not reported

calculated assuming the maximum possible surface crystallization effect.

For a heating rate of 15 K/min, our studies have shown that the DTA method is a reasonable way to determine the range of significant nucleation. However, it could be that other heating rates might not be as effective. This was tested using the numerical model by heating at half the experimental heating rate (7.5 K/min) and two times that rate (30 K/min). The diffusion coefficient obtained from the growth velocity was assumed. Figure 8 shows the calculated inverse peak temperature as a function of the nucleation treatment temperature for the three different DTA scan heating rates. Although the peak temperature shifts to a higher value with a faster heating rate and to a lower temperature for a lower heating rate, the region of significant nucleation remains the same. This indicates that the method is insensitive to the heating rate (within these limits) for the measurements, a point that to our knowledge has not been explored previously.

Evidence for the breakdown of the Stokes-Einstein equation is shown in Figure 9. The diffusion coefficient is shown as a function of temperature from experimental measurements of the viscosity[25,32,45] using the Stokes-Einstein relation, from experimental measurements of the growth velocity[25] along with Equation 7 for large nuclei, and experimental measurements of the induction time[16] using Equation 8. The diffusion coefficients obtained from the growth velocity and the induction time are in reasonable agreement, albeit on a log scale over the temperature range where experimental data are available. However, the diffusion coefficient from the viscosity and the Stokes-Einstein relation is dramatically different. Assuming that

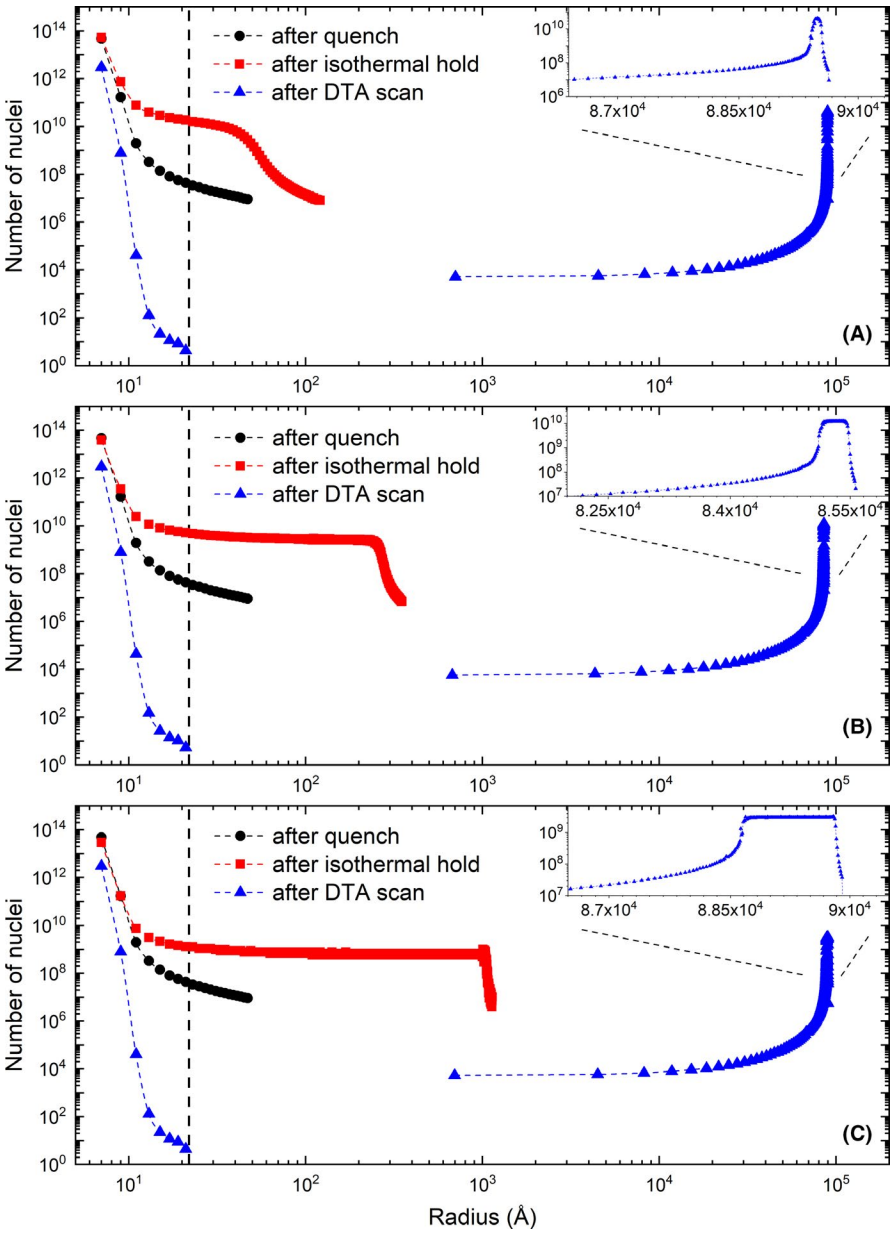

FIGURE 10 The nuclei distribution at the end of each step in a DTA simulation using the CNT, the Turnbull approximation for the driving free energy, and the diffusion coefficient from the growth velocity. The isothermal hold temperatures were (A) 970 *K*, (B) 985 *K*, and (D) 1000 *K*. Each data point represents the number of nuclei per mol in a bin of width 2 Å. Because the density of data points increases with increasing radius on the log plot, insets are shown of the nuclei distribution after the DTA scan for large radii. The vertical black dashed line is the cutoff between clusters grown by the bimolecular reaction and nuclei grown by eq. 7 at 10 r^* (10 times the critical size)

the growth velocity and induction time measures of the diffusion coefficient are correct, these data show that the Stokes-Einstein relation breaks down near 1140 K (1.18 T_g) as suggested by Rodrigues et al[25] The crystallization peaks in the DTA simulations occur between 1120K and 1150K, so the majority of the crystallization occurs in the region where the Stokes-Einstein equation is not valid. This is the cause of the error seen in Figure 5C, where the peak of the inverse peak temperature of the experimental data does not match that from the simulated data using the Stokes-Einstein relation.

The reasonable agreement found between the diffusion coefficient obtained from the growth velocity and the induction time at low temperatures in barium disilicate is in disagreement with the $Li_2O•2SiO_2$ data reported by Nascimento et al[24] and the binary $Li_2O•2SiO_2$ – $BaO•2SiO_2$ data reported by Fokin et al,[46] where the diffusion coefficient from the Stokes-Einstein relation is shown to better match with the diffusion coefficient obtained from the induction time. However, as in the manuscripts by Nascimento and Fokin, the diffusion coefficient obtained from the measured growth velocity is larger than the one obtained from the Stokes-Einstein relation at low temperatures and matches better at high temperatures. Additionally, the reasonable agreement between the diffusion coefficient from the growth velocity and induction time disagrees with the activation energy data found for $2Na_2O•CaO•3SiO_2$ by Kalinina et al.[47] However, in the paper for the soda-lime-silica glass, the temperature range for determining the activation energy is less than 100 K and the temperature range is not the same between the growth velocity, induction time, and viscosity. Given that it is widely understood that the Stokes-Einstein relation fails at lower temperatures, the agreement between the viscosity and the induction time in these other glasses is puzzling. However, the agreement between the diffusion coefficient obtained from the growth velocity and the induction time in barium disilicate, where it is not necessary to invoke the Stokes-Einstein relation, is certainly more understandable.

The ability to numerically simulate heating schedule for nucleation in a glass provides an important tool for engineers and industrial scientists seeking to develop glasses or glass ceramics with specific properties. Using the simulation presented here, it becomes possible to determine the heating schedule required to develop specific cluster and nuclei distributions. The nuclei distributions at the end of each step in the DTA simulation for the $BaO•2SiO_2$ glass for one isothermal hold temperature below, at, and above the maximum nucleation rate temperature are shown in Figure 10. This illustrates creation of as-quenched nuclei, then the development of nuclei during the isothermal hold, and finally the growth of the nuclei during the DTA scan.

4 | CONCLUSIONS

A numerical model that takes into account time-dependent nucleation during nonisothermal heating treatments was used to quantitatively model differential thermal analysis (DTA) data in a $BaO•2SiO_2$ glass. Two nucleation models were assumed for the calculations, the classical theory of nucleation (CNT) and the diffuse interface theory (DIT). Earlier experimental studies in this glass showed that the inverse peak temperatures of a DTA scan made after a series of isothermal nucleation treatments at different temperatures gave an accurate measure of the range of significant nucleation. The calculated DTA scans assuming the CNT and the DIT confirm this. For both the CNT and the DIT, good agreement with the experimental data is obtained if the diffusion coefficient is calculated from the growth velocity or the induction time. However, if the viscosity and the Stokes-Einstein relation are used to calculate the diffusion coefficient, the numerical results deviate markedly from the experimental data, demonstrating a breakdown of this relation. For the sizes of particles studied in this work, the numerical simulations show that surface crystallization does not play a role in determining the peak crystallization temperature during a DTA scan. The numerical model was used to investigate for the first time (to our knowledge) the sensitivity of the DTA technique to the scan rate. While the actual crystallization peak temperature changes as a function of scan rate, the temperature range for significant nucleation remains the same, demonstrating more broadly the validity of the DTA method.

ACKNOWLEDGMENTS

This research was partially supported by the National Science Foundation under grant DMR 17-20296 and by Corning Inc

ORCID

D. C. Van Hoesen https://orcid.org/0000-0002-4743-7993
Matthew E. McKenzie https://orcid.org/0000-0001-9091-118X
K. F. Kelton https://orcid.org/0000-0001-9857-9791

REFERENCES

1. Kelton KF, Greer AL. Crystallization in Glasses. Nucleation in Condensed Matter Applications and Materials and Biology. Oxford: Elsevier. 2010;279–329.
2. Kelton KF. Estimation of the nucleation rate by differential scanning calorimetry. J Am Ceram Soc. 1992;75(9):2449–52.
3. Ray CS, Day DE. Nucleation and crystallization in glasses as determined by DTA. J Am Ceram Soc. 1993;30:207–23.
4. Ray CS, Day DE. Determining the nucleation rate curve for lithium disilicate glass by differential thermal analysis. J Am Ceram Soc. 1990;73(2):439–42.

5. Xia X, Dutta I, Mauro JC, Aitken BG, Kelton KF. Temperature dependence of crystal nucleation in BaO.2SiO2 and 5BaO.8SiO2 glasses using differential thermal analysis. J Non Cryst Solids. 2017;459:45–50.
6. Ray CS, Fang X, Day DE. New method for determining the nucleation and crystal-growth rates in glasses. J Am Ceram Soc. 2000;83(4):865–72.
7. Ranasinghe KS, Ray CS, Day DE. A generalized method for determining the crystal nucleation and growth rates in glasses. J Mater Sci. 2002;37(1):547–55.
8. Fokin VM, Cabral AA, Reis RMCV, Nascimento MLF, Zanotto ED. Critical assessment of DTA-DSC methods for the study of nucleation kinetics in glasses. J Non Cryst Solids. 2010;356:358–67.
9. Kelton KF, Narayan KL, Levine LE, Cull TS, Ray CS. Computer modeling of non-isothermal crystallization. J Non Cryst Solids. 1996;204:13–31.
10. Ray CS, Day DE, Huang W, Narayan KL, Cull TS, Kelton KF. Non-isothermal calorimetric studies of the crystallization of lithium disilicate glass. J Non Cryst Solids. 1996;204:1–12.
11. Gránásy L. Diffuse interface theory of nucleation. J Non Cryst Solids. 1993;162(3):301–3.
12. Gránásy L. Diffuse interface approach to vapor condensation. Europhys Lett. 1993;24(2):121–6.
13. Spaepen F. Homogeneous nucleation and the temperature dependence of the crystal melt interfacial tension. In: Ehrenreich H, Turnbull D, editors. Solid State Phys. New York: Academic Press, 1994; p. 1–32.
14. Abyzov AS, Fokin VM, Rodrigues AM, Zanotto ED, Schmelzer JWP. The effect of elastic stresses on the thermodynamic barrier for crystal nucleation. J Non Cryst Solids. 2016;432:325–33.
15. Fokin VM, Abyzov AS, Zanotto ED, Cassar DR, Rodrigues AM, Schmelzer JWP. Crystal nucleation in glass-forming liquids: Variation of the size of the "structural units" with temperature. J Non Cryst Solids. 2016;447:35–44.
16. Xia X, Van Hoesen DC, McKenzie ME, Youngman RE, Gulbiten O, Kelton KF. Time-dependent nucleation rate measurements in BaO•2SiO2 and 5BaO•8SiO2 glasses. J Non Cryst Solids. 2019;525:119575.
17. Kelton KF, Greer AL, Thompson CV. Transient nucleation in condensed systems. J Chem Phys. 1983;79(12):6261–76.
18. Kelton KF, Greer AL. Transient nucleation effects in glass formation. J Non Cryst Solids. 1986;79:295–309.
19. Kelton KF. Crystal nucleation in liquids and glasses. Solid State Phys. 1991;45:75–177.
20. Kelton KF. Numerical model for isothermal and non-isothermal crystallization of liquids and glasses. J Non Cryst Solids. 1993;163:283–96.
21. Levine LE, Narayan KL, Kelton KF. Finite size corrections for the Johnson-Mehl-Avrami-Kolmogorov equation. J Mater Res. 1997;12(1):124–32.
22. Bagdassarian CK, Oxtoby DW. Crystal nucleation and growth from the undercooled liquid: a nonclassical piecewise parabolic free-energy model. J Chem Phys. 1994100(3):2139–48.
23. Kelton KF, Greer AL. The Classical Theory. Nucleation in Condensed Matter Applications and Materials and Biology. Oxford: Elsevier. 2010;19–54.
24. Nascimento MLF, Fokin VM, Zanotto ED, Abyzov AS. Dynamic processes in a silicate liquid from above melting to below the glass transition. J Chem Phys. 2011;135(19):194703.
25. Rodrigues AM, Cassar DR, Fokin VM, Zanotto ED. Crystal growth and viscous flow in barium disilicate glass. J Non Cryst Solids. 2018;479:55–61.
26. Kashchiev D. Solution of the non-steady state poblem in nucleaiton kinetics. Surf Sci. 1969;14(1):209–20.
27. Johnson WA, Mehl RF. Reaction Kinetics in Processes of Nucleation and Growth. Am Inst Min Metall Eng. 1939;135:416–442.
28. Avrami M. Kinetics of phase change. I general theory. J Chem Phys. 1939;7(12):1103–12.
29. Avrami M. Kinetics of phase change. II transformation-time relations for random distribution of nuclei.J Chem. 1940;8(2):212–24.
30. Avrami M. Granulation, phase change, and microstructure kinetics of phase change. III. J Chem Phys. 1941;9(2):177–84.
31. Kolmogorov AN. A statistical theory for the recrystallization of metals. Izu Akad Nauk SSSR. 1937;3:355–359.
32. Zanotto ED, James PF. Experimental tests of the classical nucleation theory for glasses. J Non Cryst Solids. 1985;74:373–94.
33. James PF, Rowlands EG. Kinetics of crystal nucleation and growth in barium disilicate glass. Phase Transform. Vol. 2. London: The Institution of Metallurgists, Northway House, 1979; p. 27–9.
34. Fokin VM, Kalinina AM, Filipovich VN. Nucleation in silicate glasses and effect of preliminary heat treatment on it. J Cryst Growth. 1981;52:115–21.
35. Deubener J, Brückner R, Sternitzke M. Induction time analysis of nucleation and crystal growth in di- and metasilicate glasses. J Non Cryst Solids. 1993;163(1):1–12.
36. Barker MF, Wang T-H, James PF. Nucleation and growth kinetics of lithium disilicate and lithium metasilicate in lithia-silica glasses. Phys Chem Glas. 1988;29(6):240–8.
37. Kivelson D, Kivelson SA, Zhao X, Nussinov Z, Tarjus G. A thermodynamic theory of supercooled liquids. Phys A. 1995;219:27–38.
38. Tarjus G, Kivelson SA, Nussinov Z, Viot P. The frustration-based approach of supercooled liquids and the glass transition : a review and critical assessment. J Phys Condens Matter. 2005;17(50): R1143–82.
39. Nussinov Z. Avoided phase transitions and glassy dynamics in geometrically frustrated systems and non-Abelian theories. Phys Rev B. 2004;69(1).
40. Xiaojie JX, Chandra SR, Delbert ED. Nucleation and crystallization of Na2O. 2CaO. 3Si02 glass by differential thermal. Analysis. J Am Ceram Soc. 1991;14:909–14.
41. Abyzov AS, Fokin VM, Yuritsyn NS, Rodrigues AM, Schmelzer JWP. The effect of heterogeneous structure of glass-forming liquids on crystal nucleation. J Non Cryst Solids. 2017;462:32–40.
42. Gupta PK, Cassar DR, Zanotto ED. Role of dynamic heterogeneities in crystal nucleation kinetics in an oxide supercooled liquid. J Chem Phys. 2016145(21):211920.
43. Schmelzer JWP, Abyzov AS. Crystallization of glass-forming liquids: thermodynamic driving force. J Non Cryst Solids. 2016;449:41–9.
44. Cassar DR, Serra AH, Peitl O, Rodrigues AM, Zanotto ED. The Failure of the Classical Nucleation Theory at Low Temperatures Resolved. arXiv:190203193v1. 2019.
45. Lenoir M, Grandjean A, Linard Y, Cochain B, Neuville DR. The influence of Si, B substitution and of the nature of network-modifying cations on the properties and structure of borosilicate glasses and melts. Chem Geol. 2008;256:316–25.
46. Fokin VM, Abyzov AS, Rodrigues AM, Pompermayer RZ, Macena GS, Zanotto ED, et al. Effect of non-stoichiometry on

the crystal nucleation and growth in oxide glasses. Acta Mater. 2019;180:317–28.

47. Kalinina AM, Filipovich VN, Fokin VM. Stationary and non-stationary crystal nucleation rate in a glass of 2Na2O.CaO.3SiO2 stiochiometric composition. J Non Cryst Solids. 1980;38 & 39:723–8.

How to cite this article: Van Hoesen DC, Xia X, McKenzie ME, Kelton KF. Modeling nonisothermal crystallization in a $BaO{\bullet}2SiO_2$ glass. *J Am Ceram Soc*. 2019;00:1–12. https://doi.org/10.1111/jace.16979